Available online at www.sciencedirect.com

ScienceDirect

Ceramics International 41 (2015) 4531–4537

CERAMICS INTERNATIONAL

www.elsevier.com/locate/ceramint

Synthesis and fabrication of novel cuttlefish (*Sepia officinalis*) backbone biografts for biomedical applications

Bunyamin Aksakal[a,*], Mehtap Demirel[b]

[a]*Yildiz Technical University, Faculty of Chemical and Metallurgy, Dept Metallurgy and Mater Eng. Istanbul, Istanbul, Turkey*
[b]*Adiyaman University, Vocational School of Technical Sci, Adiyaman, Turkey*

Received 29 October 2014; received in revised form 27 November 2014; accepted 27 November 2014
Available online 5 December 2014

Abstract

New biografts were fabricated via the sol–gel method by using different proportions of cuttlefish (*Sepia officinalis*) backbone and hydroxyapatite powder (HAp). The effect of the different proportions of cuttlefish (CF) on the morphology, mechanical properties and microstructure of the micro and nano scale-HAp were studied. Chemical properties and phase transformations of the fabricated biografts were characterized by SEM, XRD and FTIR analysis. Mechanical properties of the produced grafts were examined by hardness and compression tests. The results showed that crystallinity of the grafts increased with the increasing CF proportions. No significant difference was detected in its strength by changing the particle size of HAp e.g. micro and nano scale-HAp with different proportions of CF backbone. However, porosity and sinterability of the fabricated grafts were noted to increase and cracks on the surface decreased with increasing the CF backbone amount. Also, micro scale-HAp based biografts produced a higher hardness than the nano scale-HAp based biografts. The highest hardness was obtained from the biograft samples containing 40% micro scale-Hap.

Keywords: Bone graft; Hydroxyapatite; Cuttlefish backbone

1. Introduction

Bioceramics are used in diseased and/or defective parts of the hard tissues in the human body [1]. Calcium phosphate containing ceramics are especially known to be a promising materials due to their excellent biocompatibility [2]. Hydroxyapatite (HA) is one of the most conventional bioceramics which are biocompatible and the main component is bone. It has a broad area of use because of its ability to maintain good bonding between bone and its surrounding tissue [3,4]. HAp has an important role in materials chemistry since it has excellent biocompatibility and good chromatographic properties to refine proteins [5,6]. However, the lack of mechanical properties of HAp is probably the only disadvantage of this material [7]. In order to improve its mechanical properties and the biological properties of HAp, a vast number of studies have been conducted over the last 20 years [5,8–11,13]. In this context, as an alternative, Sea-derived natural fish skeletons are also used as calcium phosphate sources due to their structural resemblance to human bone [12–15].

Cuttlefish backbone is a lightweight cellular material and has two main components, the dorsal shield and the lamellar matrix. The dorsal shield is very tough and dense providing a rigid substrate and a lamellar matrix of CF [16,17]. Cuttlefish backbone has been proposed as a suitable raw material for a range of applications. For instance, Poompradub et al. [18] investigated the potential use of cuttlefish backbone as a filler of natural rubber. Even though it was significantly less refined, it was reported that the cuttlefish backbone had comparable mechanical properties to commercially available bone graft fillers. Yildirim et al. [19] investigated a quantitative analysis of mineral substances in raw cuttlefish backbone. They reported that the mineral composition of cuttlefish backbone is similar to human bone tissue but they suggested that the direct use of cuttlefish backbone as a bone tissue scaffold warranted further investigation.

In recent years, the studies on calcium phosphates applications and the usage of these materials in healthcare increased due to its high biocompatibility in the body. Such materials are

*Corresponding author.
E-mail address: baksakal@yildiz.edu.tr (B. Aksakal).

http://dx.doi.org/10.1016/j.ceramint.2014.11.148
0272-8842/

reported to be more suitable for high loading applications [20]. CF backbone is a material which is cost efficient and easy to obtain. Also CF contains porous $CaCO_3$ and Calcium phosphate ($Ca–PO_4$) structures exhibiting bone like ions. Due to its resemblance to bone structure and because of its composition, crystallinity, pore size and biocompatibility, as it is a natural material, CF backbone can be used as alternative biograft in defected bones [21–23]. Depending on these properties of HAp and CF, micro and nano scale HAp based-CF containing M-H30S20, M-H30S30, M-H30S40 and N-H30S20, N-H30S30, N-H30S40 were synthesized via the sol–gel method and its chemical, morphological and mechanical properties were investigated.

In this study, novel bone grafts were synthesized by the addition of different proportions of CF and sol–gel additives (P_2O_5, Na_2CO_3, KH_2PO_4 and CaO) into both micro and nano scale HA powders. The crystallinity, composition, structures and mechanical properties were characterized by X-ray, FTIR and SEM analysis, respectively. It was shown via SEM images that the grafts have high densification structure and varying hardness and strengths depending up on CF concentration ratios.

2. Experimental

In the present study, nano scale (< 200 nm) (Sigma; 1306-06-5) and micro scale (25 μm) HA ($Ca_{10}(PO_4)_6(OH)_2$) (Merck; LR 290280 L41) and micro scale CF were used as main components of the biografts. As for the sintering additive, KH_2PO_4 ($> 99.5\%$ purity, Merck-1.04873.0250), Na_2CO_3 ($> 99.5\%$ purity, Sigma-497-198), CaO (95% purity, Carlo Erba-331567), P_2O_5 (97.1% purity, Merck-K33152940.418) were used.

CF was provided from Mersin, Turkey (along the coast of the Mediterranean Sea). The CF was washed and dried under vacuum conditions, then mechanically ground in a grinder using alumina balls. The powder particle size was reduced to 14 μm. The obtained CF powder was kept in alcohol for 48 h and then dried in an oven for 28 h at 70 °C. The ground CF powders were homogeneously mixed with HA powder and other additives such as: Na_2CO_3, CaO, P_2O_5 and KH_2PO_4. Then, as shown in Fig. 1, the same proportions of these additives (CaO, KH_2PO_4, Na_2CO_3 P_2O_5) and different proportions of CF (20, 30 and 40%) were added to the micro and nano scale-HA powders and homogeneously mixed using an ultrasonic homogenizer. The obtained gel was then left to dry at 120 °C at normal atmosphere for 24 h. After completely drying, the powders were isostatically compacted and sintered at 1180 °C for 2.5 h in a vacuum. The fabricated grafts were characterized with an X-ray diffractometer, XRD, (BRUKER D8 ADVANCE ($\lambda = 15406$ Å), Fourier transformation infrared spectrometer, FTIR FTIR spectrums were obtained at 4000–400 cm^{-1} range (ALTI Unicam WATTSON 1000) and structural images by scanning electron microscope, SEM (JEOL JSM-7001F). The compression strengths of produced grafts were evaluated with a universal testing machine (Shimadzu, Autograph, 5 kN) at 5 mm/min interval. For the hardness tests, three cylindrical discs for each group (micro-scale HA and nano-scale HA and 20–40% CF doped) specimens having a 10 mm diameter and 1 mm height were prepared. Hardness measurements of the fabricated CF dopped biograft samples were executed on a Future Tech, FM-700 tester with a Vickers pyramid tip under 20 N loading for 5 s time intervals.

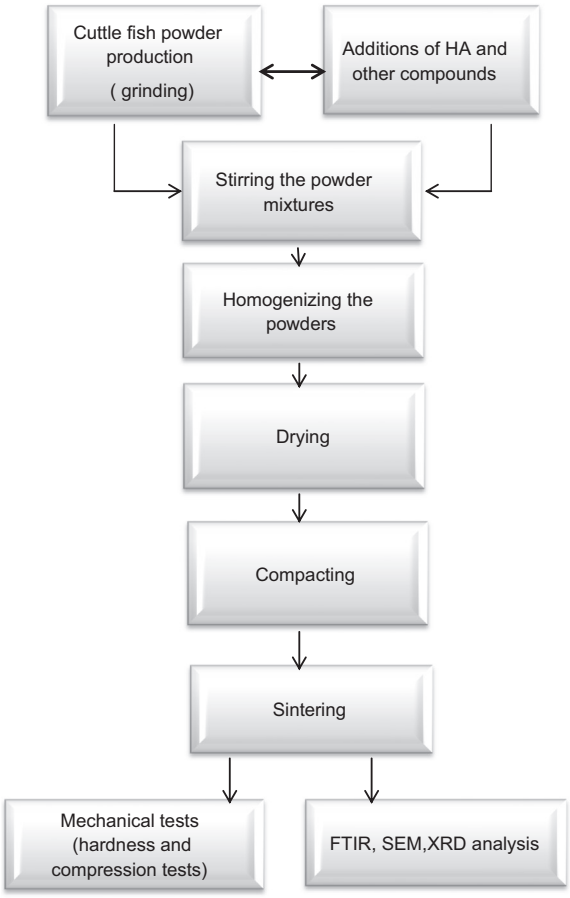

Fig. 1. Experimental flow chart of biograft fabrication process.

3. Results

HAp based CF grafts with ratios between 20 and 40% were synthesized via the sol–gel method. During the synthesis, the additives KH_2PO_4, Na_2CO_3, P_2O_5, CaO were added to increase gelation, densification and sintering properties. The effects of micro and nano scale-HA and different proportions of CF were investigated for 20, 30, and 40% CF additions. Fig. 2a shows the FTIR spectra of the CF containing and micro scale-HA based biografts. The result of using the concentrations (20, 30, 40%) CF ratios and micro scale HAp, a broad and low intensity $(CO_3)^{2-}$ peaks at 2987.53 cm^{-1} was observed. Also at 1167.77–977.32 cm^{-1} intervals and 1023.63 cm^{-1}, a sharp $(PO_4)^{3-}$ peak is seen (Fig. 2a). The results of the biografts produced at 20–30% CF concentration ratios with nano-scale HAp were shown in Fig. 2b. The peak $(PO_4)^{3-}$ is seen at 1086.87–962.78 cm^{-1} intervals. When the micro and nano scale-HA based biografts are compared, the peaks for the nano scale HA based biografts are sharper and narrower. In addition, $(CO_3)^{2-}$ the peak of micro scale HAp based biografts were also observed for nano scale-HA based biografts.

Fig. 3a shows the XRD spectra of the micro scale-HA based, 20, 30, 40% CF concentration rates as M-H30S20, M-H30S30 and M-H30S40 biografts. XRD patterns of nano

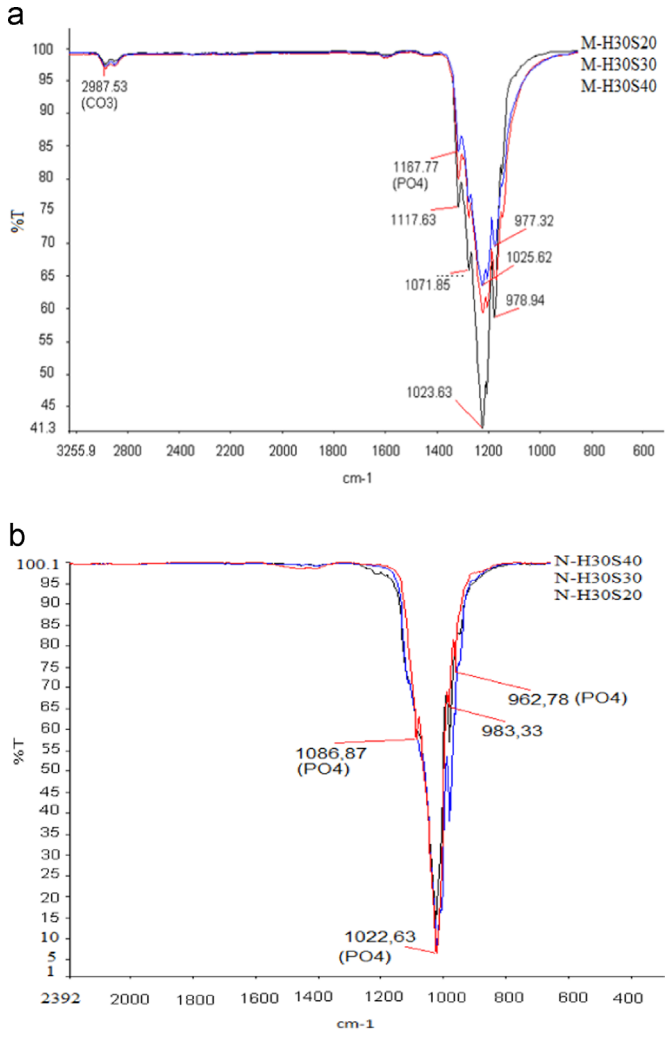

Fig. 2. FTIR spectra for (a) micro and (b) nano scale-CF containing biografts.

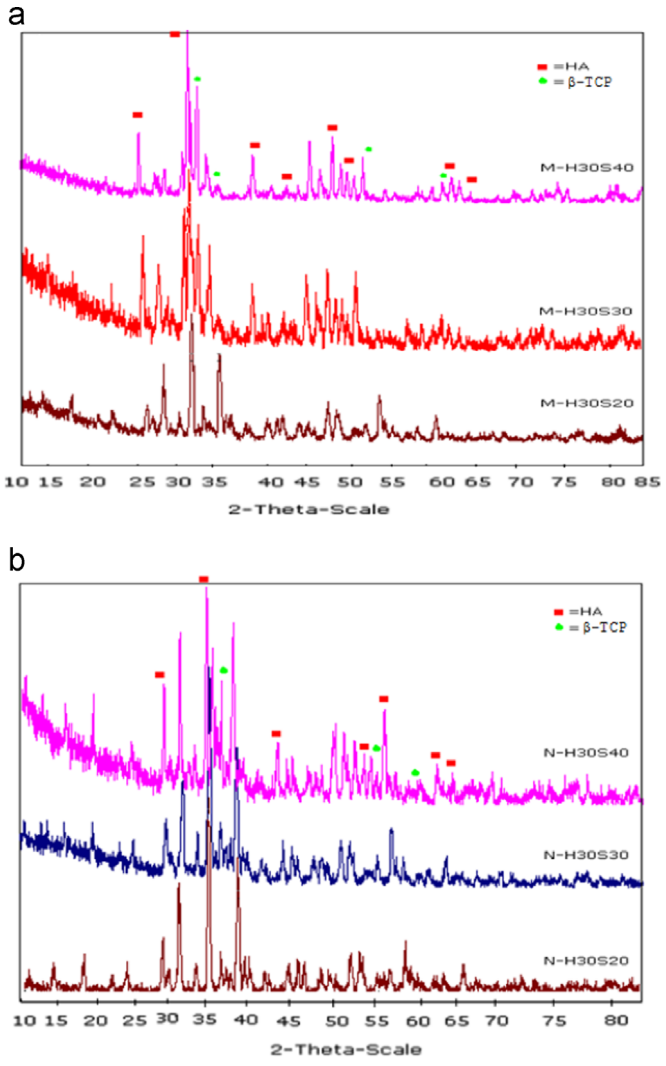

Fig. 3. XRD patterns for micro scale-HA (a) M-H30S20, M-H30S30 and M-H30S40 and nano scale-HA (b) N-H3SL20, N-H30S30 and N-H30S40.

scale-HA based with 20, 30, 40% CF concentration rates and N-H30S20, N-H30S30 and N-H30S40 are shown in Fig. 3b. SEM images at × 5000 magnification of the micro-scale HA based and 20–40% CF added biografts were shown in Fig. 4a–c. SEM images of the three different grafts at × 5000 magnifications for 30% micro scale-HA based, 20% of CF (M-H30S20) for 30% CF (M-H30S30) and for 40% CF(M-H30S40) additions are shown in Fig. 4a–c, respectively. As a consequence of the liquid phase sintering at 1180 C, an ordered grain distribution and small apatite agglomerations on the surface can be observed in Fig. 4b.

In order to show the effects of HAp particle sizes, the nano and micro-scale HA grains and apatite minerals inside the bone, the studies on particle sizes such as micro and nano-scale HA are drawing attention in the biomaterials research area [24,25]. In this study, by the addition of various natural powders such as CF, the structure of the obtained grafts were investigated and SEM images of nano scale-HA based and 20–40% CF backbone containing biografts are shown in Fig. 5a–c. SEM images corresponding to 30% nano scale-HA based and 20% CF powder added (N-H30S20) biografts are given in Fig. 5a. 30% CF powder was added (N-H30S30) in Fig. 5b and 40% CF powder was added (N-H30S30) in Fig. 5c, respectively. According to the SEM images shown in Fig. 5c, due to liquid phase sintering, grain boundaries in the N-H30S40 are not seen clearly and because of the usage of HA, some agglomerated apatite particles are present. Also surface cracks at the grain boundaries can be seen at the surface of the N-H30S40. On the other hand, SEM images of N-H30S20 and N-H30S30 show that the N-H30S40 sample is the only graft that has unclear grain boundaries and surface cracks. Compression tests were performed for micro scale HA based-CF added M-H30S20, M-H30S30, M-H30S40. The Stress-elongation (%) graph is shown in Fig. 6a–c. Vickers micro hardness results for micro and nano scale-HA based-CF added biografts are given in Fig. 7.

4. Discussion

4.1. FTIR

Due to the known facts that the cuttle fish bone is dissolved in H_3CO_3, few studies have been conducted to show the

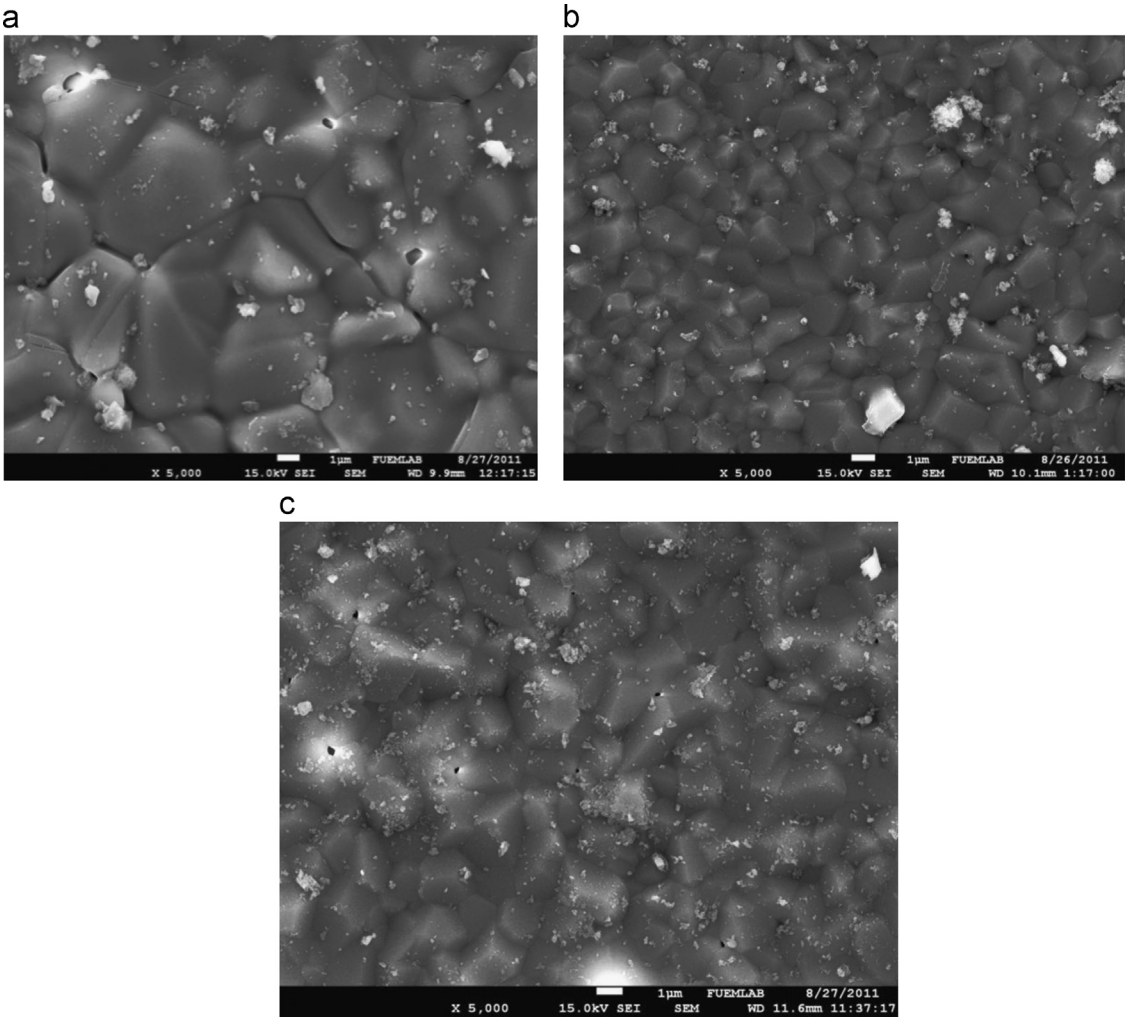

Fig. 4. SEM images of (a) M-H30S20, (b) M-H30S30 and (c) M-H30S40.

reaction changes [26] and sinterability [27]. In the current work, differing from current literature, the effects of wt% cuttle fish additions into HA and changes in structure and mechanical properties were focused on. As a result of FTIR analysis, as reported in [28], the PO_4^{3-} peak seen between 962.78 and 1167.77 cm^{-1} intervals were determined in response to HAp and the CF powder. Due to the $CaCO_3$ compound in the CF powder for M-H30S20, M-H30S30 and M-H30S40, CO_3^{2-} peak at 2987.53 cm^{-1} is detected at micro-scale-HA biografts (Fig. 2a).

In addition, it was seen that as the CF powder proportions increase in micro scale-HA based biografts, the sharpness of the peak also increases and the sharpest peak was obtained at 40% CF containing biografts. On the contrary, in the nano scale HAp based and 20–40% CF containing biografts, as the CF amount decreases, the sharpness of the peak increases (Fig. 2b). When all the micro and nano scale HAp based-CF added biografts are compared, and due to the presence of HA and CF backbone powder, PO_4^{3-} and CO_3^{2-} peaks were detected. On the other hand, peaks of nano scale-HA based biografts are noticed to be sharper and narrower. The CO_3^{2-} peak in the nano-scale HA based biografts are absent as shown in Fig. 2b. Therefore, it is possible to synthesize such biografts with improved biocompatibility and mechanical properties as reported in [20].

4.2. XRD analysis

The XRD analysis showed that sharper peaks seen between 2θ degrees of 25° and 40° correspond to HA and β-TCP phases, respectively (Fig. 3a and b). According to the analysis, all biografts show the same peaks at similar patterns, while there was no phase change with increasing CF amounts. As CF amounts increases from 20% to 30%, there was no significant change in peak width but the increase in the peak length. Also compared to other biografts, in 40% CF containing N-H30S20 and N-H30S30 peak widths seem to be remarkably decreased, peak length has increased and HA and β-TCP phases are formed. Formation of small amounts of β-TCP is advantageous as it allows ionic substitutions and thereby may enhance bioactivity of the material [28]. In the case of the HA phase and β-TCP, grain behavior of β-TCP was similar with [29,30].

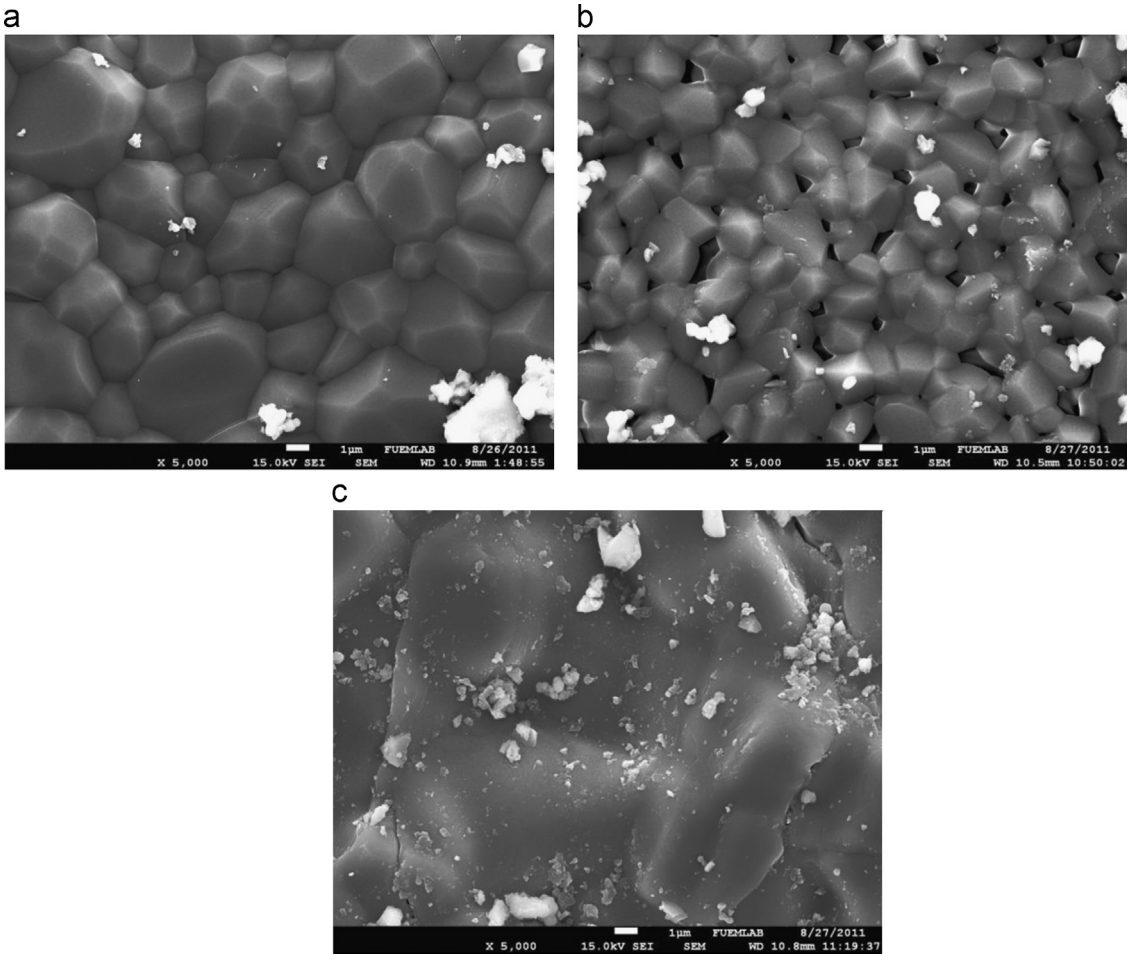

Fig. 5. SEM images of (a) N-H30S20, (b) N-H30S30 and (c) N-H30S40 biografts.

Various researchers also reported that some sintering aids to promote formation of other phases like α- and β-TCP, the amount and the rate being dependent on sintering temperatures and the compositions of the sintering additives [31–33].

4.3. SEM analysis

From the SEM images shown in Figs. 4 and 5, the biografts present a uniform grain distribution due to liquid phase sintering in micro and nano scale-HA based with different proportions of CF additions (20, 30 and 40%). SEM images of M-H30S20 shows a uniform grain distribution and agglomerated HA structure and small porous particles along grain boundaries that are the initial starting points of cracks on the graft surface (Fig. 4). In addition, as shown in Fig. 4b, The M-H30S30 is free of cracks indicating a denser structure as also can be seen in [28].

The white zones around the porous structures seen in Fig. 4a belong to the agglomerated HA particles and porous structural forms which is similar to the structures published previously [27,36]. Compared to M-H30S30 and M-H30S20, in N-H30S30 there seem to be a better uniform grain formation and pore distribution (Fig. 5).

Fig. 4c shows a uniform grain distribution of M-H30S40 which has a low amount of small and ordered HA formations on the surface. Furthermore, due to partial liquid phase sintering that occurred during the sintering of M-H30S40, less grain boundaries are observed in comparison to M-H30S30 (Fig. 4b and c). In addition, a morphological structure with agglomorated particles is obtained and the N-H30S20 which was produced by nano scale-HA powder, has a more ordered grain structure in contrast to the sample M-H30S20 (Fig. 4a–c and Fig. 5a–c). On the other hand, when N-H30S30 and M-H30S30 is compared, there are no vacancies in between the grain boundaries in M-H30S30 structures and the clearance in grain boundaries is poorer.

4.4. Mechanical tests

Compression strength and hardness results were plotted in Figs. 6 and 7, respectively. Stress-elongation (%) graphs plotted for all biografts give similar tensile strengths, elastic slope and yield points. It was noted that elongation (%) values change with the CF concentration rate. M-H30S30 (30% micro scale-HA based, 30% CF added) provided the maximum elongation values. When compression strengths and hardness values of micro and nano scale-HA based-CF containing biografts are considered, it was noticed that, opposite to the

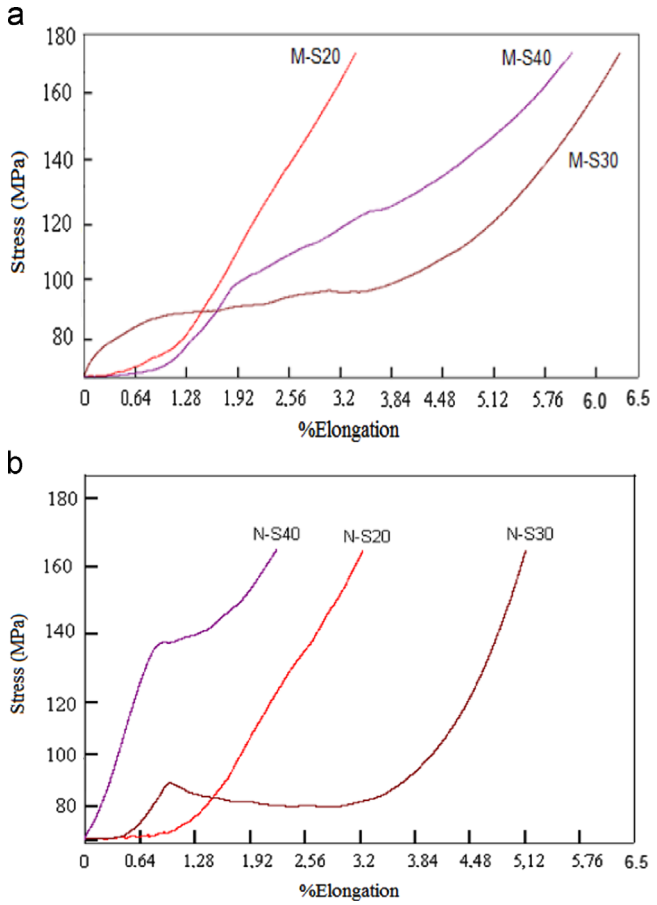

Fig. 6. Stress—elongation% curves of micro scale-HA based (a) M-H30S20, M-H30S30, M-H30S40, (b) N-H30S20, N-H30S30, N-H30S40 alternative biografts after compression test.

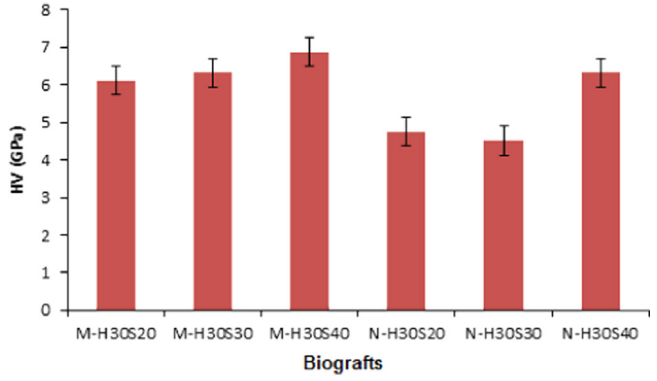

Fig. 7. Vickers hardness values of the fabricated HA based-CF containing biografts.

elongation% values, compression strength of all biografts are close to each other and hardness values are found between 4.52 and 6.87 GPa. From the compression tests, in micro and nano scale-HA based biografts with different proportions of CF, no significant changes in strength was detected with differing CF amount as the stress values are found to be between 169 and 170 MPa. Furthermore, among micro and nano scale-HA with 20, 30, 40% CF added biografts, the N-H30S30 had a 5.1% elongation as the N-H30S40 produced the lowest elongation at 2.2%. On the other hand, M-H30S40 had the highest elongation value at 24%. SEM images show a compact morphological structure with clear grain boundaries free of pores. Compression test results of nano and micro scale-HA powder particles containing CF are given in Fig. 5b. N-H30S40 seems to give the highest tensile strength while N-H30S20 gives the lowest. In comparison of the SEM images, in contrast to the compact images detected in N-H30S40, and due to liquid phase sintering, N-H30S20 shows clear grain boundaries and less agglomeration. As elastoplastic energy values that are directionally proportional to fracture strength of all nano and micro scale-HA based-CF containing biografts are compared, it can be seen that the micro scale-HA based and 40% CF containing M-H30S40 produced the highest fracture strength while micro HA based and 20% CF containing M-H30S20 has the lowest fracture strength. The compressive strengths of these obtained biografts, although some of them were related to porous ones, are higher than that reported in previous literatüre [26–28,35].

Hardness values of HA based and 20–40% CF containing biografts are given in Fig. 7. In general, it can be seen from the figure that as the hardness value increased with increasing hardness. As a result, at nano scale-HA, the highest hardness value is found for 30% HA based and 40% CF containing N-H30S40, and the lowest hardness value is found in the sample containing 30% HA and 30% CF in N-H30S30. From the comparisons, it was found that micro scale HA based biografts give higher hardness values than the nano scale-HA based biografts at various rates of CF backbone additions. The highest hardness value was obtained for the M-H30S40 (6.87 GPa) and lowest hardness value for the M-H30S20 (6.12 GPa) among micro scale-HA based CF containing biografts. On the other hand, N-H30S40 gave the highest hardness value at 6.31 GPa while N-H30S20 had the lowest hardness value of 4.75 GPA among nano scale-HA based CF containing biografts. When these values are compared to the hardness values of HA given in previous literature, it is seen that all fabricated biografts, except N-H30S20 and N-H30S30, have higher hardness values than the pure HA. The biografts obtained through the current work would be used as alternative biografts of hard tissue applications in orthopaedics [13,16,19,34]. Such biografts could also be suitable for loading human mesenchymal stem cells or transforming growth factors and bone morphogenic proteins in bone regeneration [29,30].

5. Conclusions

In this study, HA based cuttlefish (CF) backbone derived biografts are fabricated as an alternative to existing bone grafts.

- FTIR results of HA based-CF containing biografts revealed that PO_4^{3-} and CO_3^{2-} compounds were obtained and XRD results show that HA and partially β-TCP phases were formed.
- In HA based biografts, as the weight percentage of additives (except CaO, P_2O_5, KH_2PO_4 and Na_2CO_3) like CF increases, corresponding to the decrease in peak width and increase in peak length, a more crystalline structure with larger grains is obtained.

- Compression strength of HA based—CF containing biografts are close to each other, but it was observed that elongation(%) values are different and the highest elongation value was found for N-H30S30 at 5.1% and the lowest elongation value was recorded for N-H30S40 by 2.2%.
- The highest hardness value was obtained from M-H30S40 (6.87 GPa) and the lowest hardness value from M-H30S20 (6.12 GPa) among micro scale-HA based-CF containing biografts.
- The nano scale-HA based-CF containing biografts, N-H30S40 exhibits the highest hardness value (6.31 GPa) as the sample N-H30S20 producing the lowest (4.75 GPa).

References

[1] D.K. Pattanayak, R. Dash, R.C. Prasad, B.T. Rao, R. Mohan, Synthesis and sintered properties, Eval. Calcium Phosphate Ceram. Mater. Sci. Eng. C 27 (2007) 684–690.

[2] T.V. Safranova, V.I. Putlyaev, M.A. Shekhirev, Y.D. Tredyakov, A.V. Kuznetsov, A.V. Belyakov, Densification additives for hydoxapatite ceramics, J. Eur. Ceram. Soc. 29 (2009) 1925–1932.

[3] T. Kitsugi, T. Yamamuro, T. Nakamura, T. Kokubo, M. Takagi, T. Shibuya, H. Takeuchi, M. Onu, Bonding behavior between two bioactive ceramics in vivo, J. Biomed. Mater. Res. 21 (1987) 1109–1123.

[4] S. Kotani, Y. Fujita, T. Kitsugi, T. Nakamura, T. Yamamura, C. Ohtsuki, T. Kokubo, Bone bonding mechanism of beta-tricalcium phosphate, J. Biomed. Mater. Res. 25 (1991) 1303–1315.

[5] R.Z. LeGeros, Properties of osteoconductive biomaterials: calcium phosphates, Clinical Orthop. Related Res. 395 (2002) 81–98.

[6] T. Kawasaki, Hydroxapatite as a liquid chromatographic packing, J. Chromatogr. 1-2 (544) (1991) 147–184.

[7] L.L. Hench, Bioceramics: from concept to clinic, J. Am. Ceram. Soc. 74 (1991) (1487-10).

[8] G. Kawachi, S. Sasaki, K. Nakahara, E.H. Ishida, K. Ioku, Porous apatite carrier prepared by hydrothermal method, Key Eng. Mater. 309-311 (2006) 935–938.

[9] A.N. Vasiliev, E. Zlotnikov, J.G. Khinast, R.E. Riman, Chemisorption of silane compounds on hydroxapatites of various morphologies, Scr. Mater. 58-12 (2008) 1039–1042.

[10] R.A. Laudise, Growty of Single Crystals, Prentice-Hall, Inc, New Jersey, 1970.

[11] L. Jingbing, X. Ye, H. Wang, M. Zhu, B. Wang, H. Yan, The influence of pH and temperature on the morphology of hydroxapatite synthesized by hydrothermal method, Ceram. Int. 29 (2003) 629–633.

[12] D. Green, D. Walsh, S. Mann, R.O.C. Oreffo, The potential of biomimesis in bone tissue engineering: lessons from the design and synthesis of invertebrate skeletons, Bone 50 (2-3) (2002) 253–259.

[13] R. Vago, D. Plotquin, A. Bunin, I. Sinelnikov, D. Atar, D. Itzhak, Hard tissue remodeling using biofabricated coralline biomaterials, J. Biochem. Biophys. Methodol. 50 (2-3) (2002) 253–259.

[14] M. Sarikaya, J. Liu, I.A. Aksay, Properties, Crystallography, and Formation, Biomimetics: Design and Processing of Materials, American Institute of Physics, New York, 1995, p. 34–90.

[15] P. Calvert, S. Mann, Review: synthetic and biological composites formed by in-situ precipitation, J. Mater. Sci. 23 (1988) 3801–3806.

[16] J.D. Birchall, N.L. Thomas, On the architecture and function of cuttlefish bone, J. Mater. Sci. 18 (1983) 2081–2086.

[17] D. Gower, J.F.V. Vincent, The mechanical design of the cuttlebone and its bathymetric implications, Biomimetics 4 (1996) 37–57.

[18] S. Poompradub, Y. Ikeda, Y. Kokubo, T. Shiono, Cuttlebone as reinforcing filler for natural rubber, Eur. Polym. J. 44 (2008) 4157–4164.

[19] O.S. Yildirim, Z. Okumus, M. Kizilkaya, Y. Ozdemir, R. Durak, A. Okur, Comparative quantitative analysis of sodium, magnesium, potassium and calcium in healthy cuttlefish backbone and non-pathological human elbow bone, Can. J. Anal. Sci. Spectros. 52 (2007) 270–275.

[20] Z. Evis, Çeşitli iyonlar eklenmiş nano- hidroksiapatitler: Üretim yöntemleri, iç yapı, mekanik ve biyouyumluluk özellikleri yönlerinden incelenmesi, Int. J. Eng. Res. Dev. 3 (2011) 55–61.

[21] H.A. Lowenstam, S. Weiner, On Biomineralization, Oxford Univ. Press, Oxford, 1989.

[22] F. Manoli, E. Dalas, Calcium carbonate crystallization on xiphoid of the cuttlefish, J. Cryst. Growth 217 (2000) 422–428.

[23] J.D. Bobyn, R.M. Pilliar, H.U. Cameron, G.C. Weatherly, The optimum pore size for the fixation of porous-surfaces metal implants by the in growth of bone, Clin. Orthop. Related Res. 150 (1980) 263–270.

[24] B. Aksakal, B. Dikici, M. Gavgali, The effect of coating thickness on corrosion resistance of hydroxyapatite coated Ti6Al4V and 316L SS implants, J. Mater. Eng. Perform. 6 (2010) 894–899.

[25] S. Sonmez, B. Aksakal, B. Dikici, Corrosion protection of AA6061–T4 alloy by sol–gel derived micro and nano-scale hydroxyapatite (HA) coating, J. Sol–Gel Sci. Technol. 63 (3) (2012) 510–518.

[26] S.J. Lee, M.H. Lee, W.M. Kriven, N.S. Oh, Sintering behavior and biocompatibility of calcium phosphates fabricated by cuttlefish bone and phosphoric acid, J. Tissue Eng. Regen. Med. 7 (5) (2010) 556–560.

[27] S. Pankaj, L. Sang-Jin, D.A. Zlatomir, M.K. Waltraud, Porous biphasic calcium phosphate scaffolds from cuttlefish bone, J. Am. Ceram. Soc. (2011) 2362–2370.

[28] S.J. Kalitaa, S. Bosea, H.L. Hosickb, A. Bandyopadhyaya, CaO–P_2O_5–Na_2O-based sintering additives for hydroxyapatite (HAp) ceramics, Biomaterials 25 (2004) 2331–2339.

[29] S.J. Lee, Y.C. Lee, Y.S. Yoon, Characteristics of calcium phosphate powders synthesized from cuttlefish bone and phosphoric acid, J. Ceram. Process. Res. 8 (2007) 427.

[30] N.Y. Mostafa, Characterization, thermal stability and sintering of hydroxyapatite powders prepared by different routes, Mater. Chem. Phys. 94 (2005) 333.

[31] J.C. Knowles, Development of hydroxyapatite with enhanced mechanical properties: effect of glass addition on mechanical properties and phase stability of sintered hydroxyapatite, Ceramic Industr, Division Annual Convention, Brunel University, 1993 (20–23 April).

[32] M.A. Lopes, J.D. Santos, F.J. Monteiro, J.C. Knowles, Glassreinforced hydroxyapatite: a comprehensive study of the effect of glass composition on the crystallography of the composite, J. Biomed. Mater. Res. 39 (1998) 244–251.

[33] P.W. Sylvester, H.P. Birkenfeld, H.L. Hosick, K.P. Briski, Fatty acid modulation of epidermal growth factor-indu ced mouse mammary epithelial cell proliferation in vitro, Exp. Cell Res. 214 (1994) 145–153.

[34] C. Demers, C. Reggie, Hamdy K. Corsi, F. Chellat, M. Tabrizian, L. Yahia, Natural coral exoskeleton as a bone graft substitute: a review, Bio-Med. Mater. Eng. 12 (1) (2002) 15–35.

[35] K. Rezwan, Q.Z. Chen, J.J. Blaker, A.R. Boccaccini, Biodegradable and bioactive porous polymer/ınorganic composite scaffolds for bone tissue engineering, Biomaterials (2006) 3413–3431.

[36] J.H.G. Rocha, A.F. Lemos, S. Agathopoulos, P. Valério, S. Kannan, F.N. Oktar, M.F. Ferreira, Scaffolds for bone restoration from cuttlefish, Bone 37 (2005) 850–857.